J Biomol NMR (2011) 50:219–227
DOI 10.1007/s10858-011-9511-7

ARTICLE

Elucidating slow binding kinetics of a protein without observable bound resonances by longitudinal relaxation NMR spectroscopy

Kenji Sugase

Received: 27 December 2010 / Accepted: 5 May 2011 / Published online: 28 May 2011

Abstract We developed a new method to elucidate the binding kinetics k_{on} and k_{off}, and the dissociation constant K_D ($=k_{off}/k_{on}$), of protein-protein interactions without observable bound resonances of the protein of interest due to high molecular weight in a complex with a large target protein. In our method, k_{on} and k_{off} rates are calculated from the analysis of longitudinal relaxation rates of free resonances measured for multiple samples containing different concentration ratios of ^{15}N-labeled protein and substoichiometric amounts of the target protein. The method is applicable to interactions that cannot be analyzed by relaxation dispersion spectroscopy due to slow interactions on millisecond to second timescale and/or minimal conformational (chemical shift) change upon binding. We applied the method to binding of the B1 domain of protein G (GB1) to immunoglobulin G, and derived the binding kinetics despite the absence of observable bound GB1 resonances.

Keywords Binding kinetics · Dissociation constant · Longitudinal relaxation experiment · Slow exchange · Unobservable bound resonance

Introduction

Molecular recognition, observed in ligand-macromolecule interactions, such as ligand-receptor, antigen-antibody, and DNA-protein, plays an important role in biological systems (Frederick et al. 2007; Babine and Bender 1997). In addition to attempts to understand ligand-macromolecule interactions from static pictures of complex structures (Redfern et al. 2008), there is an increasing interest in investigating molecular recognition processes for protein engineering and the design of new active compounds in pharmaceutical research (Karplus 2010; Karplus and Kuriyan 2005).

A dissociation constant K_D, which is defined as the ratio of the dissociation rate k_{off} to the association rate k_{on}, is one of the most important parameters for the characterization of ligand-macromolecular interactions, in particular for screening drug candidates (Ohlson 2008). There are several biophysical instruments and techniques available for determining dissociation constants, such as Biacore and isothermal titration calorimetry (ITC). NMR is also capable of determining dissociation constants. Typically, an unlabeled ligand, such as a small compound, protein, or nucleic acid, is titrated into a stable isotope (^{13}C and/or ^{15}N)-labeled protein, and a 1D or 2D NMR spectrum of the protein at each ligand addition is measured (Fielding 2007). NMR signals appear at the population-averaged chemical shifts of the free and bound states under conditions of fast exchange on the chemical shift timescale. Dissociation constants are calculated from the curve fitting of chemical shift changes as a function of the molar ratio of a ligand to its target protein. Ligand binding sites on the target protein are also mapped in the same experiment. In some cases, two distinct dissociation constants can be derived from the NMR titration experiments if a ligand binds to two sites on a protein (Ferreon et al. 2009). As the NMR titration experiment is very simple, it has been applied to the study of a large number of ligand-macromolecule interactions. This titration method cannot, however, be applied

K. Sugase (✉)
Bioorganic Research Institute, Suntory Foundation for Life Sciences, 1-1-1 Wakayamadai, Shimamoto-cho, Mishima-gun, Osaka 618-8503, Japan
e-mail: sugase@sunbor.or.jp

to a slow-exchange interaction because free and bound resonances do not move (but change their intensities) during titration. Thus, titration curves that are used to derive dissociation constants cannot be drawn. Alternatively, for a slow-exchange interaction, the concentrations of free macromolecule [M], free ligand [L], and the macromolecule-ligand complex [ML] are calculated from the peak intensities of the free and bound states, and the dissociation constant is derived using the equation $K_D = [M][L]/[ML]$. Using this method, Latham et al. determined the K_D ($\sim$3 mM) for the interaction between an RNA aptamer and the bronchodilator drug theophylline, which is in slow exchange as evidenced by the very slow k_{on} (600 ± 57 $M^{-1}s^{-1}$) and k_{off} (1.5 ± 0.3 s^{-1}) determined using ^{1}H ZZ-exchange spectroscopy (Latham et al. 2009). For this titration method, however, the transverse relaxation rate R_2 of the bound state must be comparable to that of the free state or be known a priori; otherwise, the fraction of the bound state can be underestimated because bound resonances usually relax faster than free resonances.

Alternatively, ligand-based NMR techniques that analyze free resonances of a ligand using samples containing very small amounts of a target macromolecule, such as saturation transfer difference (Angulo et al. 2010; Mayer and Meyer 1999) and WaterLOGSY (Dalvit et al. 2000, 2001), can also be utilized to determine dissociation constants even without isotope labeling. These methods can analyze interactions with dissociation constants in the range 10^{-3}–10^{-8} M (Mayer and Peters 2003). In ligand-based NMR experiments, NMR signals of a ligand are perturbed in the bound states, and the perturbation is transferred to the free resonances of the ligand via chemical exchange. Since these NMR techniques can probe weak interactions that are difficult to detect using other instruments or techniques, they are widely used for initial drug screening, in which novel scaffolds with a weak binding affinity can be identified. The identified compounds are then optimized using, for example, combinatorial chemistry, structure-based drug design, etc (Ludwig and Guenther 2009). Ligand-based NMR techniques are suited to the analysis of fast-exchange interactions, but their applications to slow-exchange interactions are limited because magnetization perturbed in the bound state cannot be transferred to the free resonances sufficiently during NMR measurements due to slow exchange. It is therefore difficult to determine k_{on} and k_{off} rates using both ligand- and macromolecule-based NMR techniques.

Recently, Wright and co-workers, including this author, developed a method to determine dissociation constants of slow-exchange protein-protein interactions utilizing ^{15}N R_2 dispersion spectroscopy (Sugase et al. 2007a). R_2 dispersion spectroscopy can quantitate site-specific thermodynamic, kinetic parameters, and chemical shift differences between interconverting states of a protein on microsecond to millisecond timescales (Tollinger et al. 2001; Loria et al. 1999). The R_2 dispersion method derives k_{on} and k_{off} rates, and consequently K_D ($=k_{off}/k_{on}$), from the fitting of R_2 dispersion curves measured as a function of the concentration ratio of two interacting proteins. The method was applied to an intrinsically disordered protein, the phosphorylated kinase-inducible domain (pKID) of the transcription factor CREB, which binds to the KIX domain of CREB-binding protein (CBP) in slow-exchange (Sugase et al. 2007a). In addition to the determination of the site-specific K_D values of pKID, the mechanism of coupled folding and binding processes of pKID was elucidated using R_2 dispersion.

A unique property of R_2 dispersion spectroscopy is that it can probe low-populated states that are invisible to most biophysical methods. By making use of this property, the R_2 dispersion method was extended to determine k_{on}, k_{off}, and K_D values without observable bound resonances due to very low-population of the bound state (Sugase et al. 2007b). As association-dissociation processes influence the effective R_2 relaxation rates of both free and bound resonances in a concentration ratio dependent manner, the k_{on} and k_{off} rates can be derived from analyzing the R_2 dispersion profiles of free resonances measured for multiple samples containing an ^{15}N-labeled protein of interest and substoichiometric amounts of the target protein with different concentration ratios. In the R_2 dispersion experiment, the bound state of the ^{15}N-labeled protein is low-populated, thus bound resonances are unobservable. Sugase et al. (2007b) applied the method to derive the k_{on}, k_{off}, and K_D values of an intrinsically disordered protein, Asn803-hydroxylated hypoxia-inducible factor-1 (HIF-OH) binding to the transcriptional adapter zinc-binding (TAZ1) domain of CBP. ^{15}N chemical shifts of HIF-OH in the bound state were also determined in the experiment even though they were unobservable.

Although the R_2 dispersion method is a powerful technique for determining the binding kinetics of protein-protein interactions in slow exchange on microsecond to millisecond timescales, its application is limited to flexible peptides or flexible regions of proteins, such as the intrinsically disordered proteins described above. This is because R_2 dispersion spectroscopy requires large chemical shift changes that are mainly induced by conformational changes upon binding to a target molecule. Another drawback is that the R_2 dispersion method cannot analyze very slow binding events on sub-second or slower timescales because NMR signals are not perturbed enough by a very slow association-dissociation

process during the typical 20- to 40-ms relaxation delay of R_2 dispersion experiments, resulting in no R_{ex} (the excess contribution to R_2^{eff} caused by the exchange process). Therefore, it is highly difficult to elucidate very slow binding events of rigid proteins, even using the R_2 dispersion method.

In this study, we present a new method that utilizes the ^{15}N longitudinal relaxation experiment called ZZ-exchange spectroscopy (Farrow et al. 1994), to elucidate slow binding events of rigid proteins, especially in cases where bound resonances are unobservable. This method is similar to the R_2 dispersion method that was applied to HIF-OH/TAZ1 (Sugase et al. 2007b). Namely, k_{on} and k_{off} rates are derived by fitting ZZ-exchange profiles of free resonances of an ^{15}N-labeled protein in the presence of substoichiometric amounts of its target protein. An advantage of ZZ-exchange spectroscopy over R_2 dispersion spectroscopy is that it can determine slow kinetic rates on millisecond to second timescales without the requirement of chemical shift (conformational) changes upon binding. Therefore, the ZZ-exchange method can be used to determine the binding kinetics of rigid proteins. We applied the method to the binding event of the B1 domain of *Streptococcus* protein G (GB1), a rigid globular protein composed of 56 residues, to immunoglobulin G (IgG). Previous structural studies indicated that GB1 binds to each of the two heavy chains in the Fc region of IgG with little conformational change (Sauer-Eriksson et al. 1995; Gronenborn et al. 1991). Although the binding kinetics of this interaction could not be analyzed by the R_2 dispersion method, the newly developed ZZ-exchange method enabled us to determine k_{on}, k_{off}, and consequently, K_D values.

Materials and methods

Theory

ZZ-exchange spectroscopy is a longitudinal relaxation experiment for determining the auto-relaxation rates of two interconverting states and kinetic rates of forward and backward reactions at equilibrium (Farrow et al. 1994). To characterize the binding kinetics of ligand-macromolecule interactions using ZZ-exchange spectroscopy, longitudinal relaxation profiles of the free and bound states and two exchange peaks (free→bound and bound→free) of a ^{13}C- or ^{15}N-labeled ligand (or macromolecule) are analyzed simultaneously. It is essential to observe both free and bound resonances at the same time with signal intensities sufficiently high to allow for quantitation of auto-relaxation rates and exchange rates. Thus, for example, the sample would contain a half stoichiometric amount of the target macromolecule (or ligand).

The longitudinal relaxation process has two properties that are important for characterizing the binding kinetics of ligand-macromolecule interactions compared to the transverse relaxation process. The first property is that the longitudinal relaxation process is more sensitive to slow molecular motions (occurring on millisecond to second timescales) than the transverse relaxation process because longitudinal relaxation times of macromolecules are usually longer than transverse relaxation times. Therefore, longitudinal magnetizations can be perturbed longer by slow molecular motions during experimental relaxation delays before they return to the equilibrium state. The second important property of the longitudinal relaxation process is that large chemical shift changes caused by the binding of a ligand to a macromolecule are not necessary as they are in R_2 dispersion experiments, because the longitudinal relaxation process is not affected by chemical shifts (in practice, free and bound resonances should be isolated enough to quantitate their signal intensities without peak overlap). Therefore, ZZ-exchange can be exploited to elucidate the slow binding kinetics of rigid globular proteins, which cannot be analyzed by R_2 dispersion spectroscopy.

ZZ-exchange spectroscopy is not applicable to common cases where bound resonances of a ligand are unobservable due to high molecular weight of a ligand in complex with a large macromolecule or unfavorable oligomerization at high molar ratio of the macromolecule to the ligand even if the ligand of interest is a small globular protein and its free resonances are clearly observed. Nevertheless, it is often possible to obtain ZZ-exchange profiles of free resonances of small proteins with none or substoichiometric amounts of large target macromolecules. As shown by Eq. 1, the ZZ-exchange profile of the completely free state, $I_F(t)$, is identical to the longitudinal relaxation profile measured using the regular R_1 relaxation method, assuming there is no internal slow conformational rearrangement affecting the ZZ-exchange profile:

$$I_F(t) = I_F(0)\exp(-R_{1F}t) \quad (1)$$

where R_{1F} represents the auto-relaxation rate of the free state. In the presence of substoichiometric amounts of the target macromolecule, the ZZ-exchange profiles of free resonances are perturbed by the association-dissociation process in a concentration-dependent manner, as shown by Eq. 2 for a two-state exchange model ($A + B \overset{[B]k_{on}}{\underset{k_{off}}{\longleftrightarrow}} A:B$):

$$
\begin{aligned}
I_F(t) &= \frac{I_F(0)}{\lambda_+ - \lambda_-}\left[(\lambda_+ - R_{1F} - [B]k_{on})\exp(-\lambda_- t) - (\lambda_- - R_{1F} - [B]k_{on})\exp(-\lambda_+ t)\right] \\
\lambda_\pm &= \frac{1}{2}\left[R_{1F} + R_{1B} + [B]k_{on} + k_{off} \pm \sqrt{(R_{1F} - R_{1B} + [B]k_{on} - k_{off})^2 + 4[B]k_{on}k_{off}}\right] \\
[B] &= \frac{1}{2}\left[-K_D - [A]_0 + [B]_0 + \sqrt{(K_D + [A]_0 - [B]_0)^2 + 4[B]_0 K_D}\right]
\end{aligned}
\tag{2}
$$

where A and B correspond to the small protein of interest and the target large macromolecule, respectively (Farrow et al. 1994), and R_{1B} represents the auto-relaxation rate of the small protein in the bound state. The dissociation constant K_D is calculated according to the formula $K_D = k_{off}/k_{on}$. $[A]_0$ and $[B]_0$ represent the total concentrations of A and B, and [B] is the concentration of free B at equilibrium (Eisenmesser et al. 2002). When $[B]_0$ is zero, which corresponds to the completely free state of A, Eq. 2 is simplified into Eq. 1.

If a substoichiometric amount of B is mixed with A, B will exist almost entirely in the bound state, and the value of [B] will be very small, depending on K_D, $[A]_0$, and $[B]_0$. A problem encountered during analysis of a ZZ-exchange profile is that the experimentally determined concentrations $[A]_0$ and $[B]_0$ may contain some degree of errors due to experimental manipulations, which may in turn result in miscalculation of [B] and, of course, the binding kinetics. For example, when $K_D = 100$ nM, $[A]_0 = 1$ mM, and $[B]_0 = 0.1$ mM, [B] is calculated to be 1.11 pM. If the $[B]_0$ value is wrongly determined to be 0.11 mM, corresponding to 10% overestimation, [B] becomes 1.24 pM, which is 1.11 times larger than the correct value. Therefore, in order to accurately elucidate the binding kinetics, it is necessary to include the concentrations $[A]_0$ and $[B]_0$ in the fitting parameters and to globally fit ZZ-exchange profiles measured at multiple concentration ratios to Eq. 2.

ZZ-exchange experiment

Uniformly [^{2}H,^{15}N]- and [^{13}C,^{15}N]-labeled GB1 was expressed in BL21-DE3 cells grown in M9 minimal medium, and was purified to homogeneity by reverse-phase HPLC as described elsewhere (Sugase et al. 2008). Unlabeled human IgG was purchased from Sigma. Proteins were dissolved separately in NMR buffer [90% H_2O/10% D_2O, 20 mM Tris-d_{11}-acetate-d_4 (pH 4.5 at 25°C), 50 mM NaCl, 2 mM NaN_3] and concentrated. NMR samples of the [^{2}H,^{15}N]-GB1:IgG complex, in which the concentration of GB1 was kept at 200 μM while the concentration of IgG was 0, 20, 40, or 60 μM, were prepared from a single concentrated solution of each protein to ensure concentration ratio accuracy. The concentrations of GB1 and IgG were initially determined from the absorbance at 280 nm, using extinction coefficients of 9.97 and 210 $mM^{-1}\cdot cm^{-1}$, respectively, and the effective concentrations were determined from the ZZ-exchange curve fitting using Eq. 2 as described in the previous section. ZZ-exchange spectra were measured for the four [^{2}H,^{15}N]-GB1:IgG samples at relaxation delays of 0.01, 0.02, 0.04, 0.08, 0.15, 0.25, 0.5, 1.0, and 1.5 s (Farrow et al. 1994) using a Bruker BioSpin AVANCE DMX750. Three data points (0.01, 0.25, and 1.0 s) were collected in duplicate and used to estimate the absolute uncertainties and the signal-to-noise ratio for each spectrum. Spectra were acquired using (1,024 × 128) complex points in the ($t_2 \times t_1$) dimensions with eight scans per t_1 increment and 3-s recycle delays. NMR data were processed using NMRPipe (Delaglio et al. 1995), and the peak intensities of free GB1 resonances $I_F(t)$ were measured using an in-house program as the sum of the intensities for a 3 × 3 grid centered on the peak maxima. The $I_F(t)$ curves were fitted to Eq. 2 for a two-state exchange model ($GB1 + IgG\ Fc \overset{[IgG\ Fc]k_{on}}{\underset{k_{off}}{\longleftrightarrow}} GB1 : IgG\ Fc$) using the program GLOVE (Sugase et al. 2007a, b). All residues were restricted to share the same total concentrations of $[GB1]_0$ and $[IgG\ Fc]_0$ (=2 × $[IgG]_0$ as IgG has two Fc fragments), k_{on} and k_{off} rates whereas auto-relaxation rates R_{1F} and R_{1B} were fitted locally for each residue. The goodness of fit was assessed by the reduced χ^2 value (χ^2 divided by the degrees of freedom).

Isothermal titration calorimetry experiments

Titration of IgG (150 μM) into GB1 (37 μM) was performed at 25°C using a VP-ITC titration calorimeter (MicroCal, Inc.). Two 5 μl injections of IgG solution were followed by 28 injections of 10 μl of IgG. Integration of the thermogram and subtraction of the blanks using the ITC data analysis software Origin 5.0 (MicroCal) yielded a binding isotherm that fit a one-site interaction model in which one GB1

molecule binds to one IgG Fc fragment. A nonlinear least-squares curve-fitting algorithm was used to determine the stoichiometric ratio, the dissociation constant K_D, and the change in enthalpy ΔH of the interaction. The change in entropy ΔS was then indirectly determined according to $-RT \ln (1/K_D) = \Delta G = \Delta H - T\Delta S$, where R represents the gas constant, T represents the absolute temperature, and ΔG represents the free energy change from the free to bound states. The ITC experiments were performed in duplicate to estimate the experimental error.

Results and discussion

Since GB1 is a small rigid protein, all backbone resonances of GB1 in the free state were clearly observed and were assigned in a straightforward manner (Fig. 1). On the other hand, bound GB1 resonances were unobservable or very broad due to the high molecular weight ($\sim$160 kDa) of the GB1–IgG complex and high viscosity caused by an additional interaction, which was observed in the ITC experiment as well only in the presence of excess IgG (see below). These results highlight the difficulty of analyzing the GB1–IgG interaction using conventional NMR techniques. For the GB1/IgG samples used in the ZZ-exchange experiments, we confirmed that diffusion coefficients, or viscosities, of free GB1 did not change using DOSY experiments (date not shown).

In order to elucidate the binding kinetics of the GB1-IgG interaction, we measured the ZZ-exchange of the free GB1 resonances of four NMR samples, each with a different [^{2}H,^{15}N]-GB1:IgG concentration ratio. There was no difference in the chemical shifts of the free GB1 resonances among the four samples (data not shown), and the intensities $I_F(0)$ decreased with the fraction of the free state as the amount of IgG increased. Thus, free GB1 was in slow exchange with the IgG-bound state on the chemical shift timescale. ZZ-exchange curves for all four samples were fit to Eq. 2 as a global association-dissociation process in which k_{on}, k_{off}, and the concentrations of GB1 and IgG were treated as global parameters for all residues (Fig. 2). For curve fitting, a fitting parameter for the concentration of GB1 was shared by all the samples, while a single fitting parameter was specified for the concentration of IgG for the 1:0.1 (=GB1:IgG) concentration ratio sample, and the value was scaled automatically in the fitting process by 0, 2, and 3 for the 1:0, 1:0.2, and 1:0.3 concentration ratio samples, respectively. The ZZ-exchange curves for all four samples were also fit to the Eq. 1 because their shapes appeared to be consistent with those expected from a regular R_1 experiment. Namely, it might be possible that the

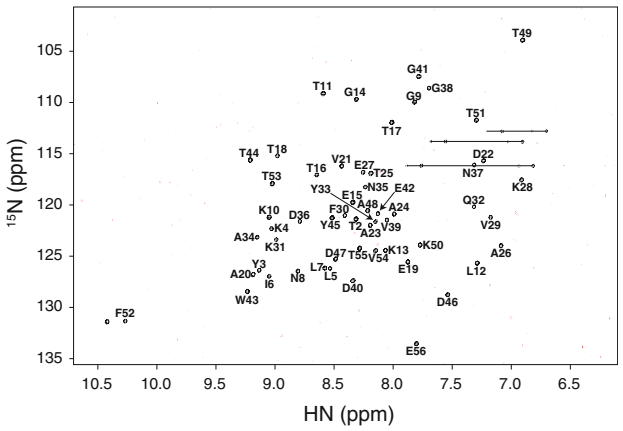

Fig. 1 ^{1}H-^{15}N clean TROSY spectra measured using a Bruker BioSpin AVANCE DMX750 spectrometer at 25°C for 200 μM [^{2}H,^{15}N]-GB1 (*black*) and 270 μM [^{15}N]-GB1 with 400 μM IgG (*red*). The TROSY spectra (Schulte-Herbrüggen and Sørensen 2000; Pervushin et al. 1997) were acquired with 2 scans per t_1 increment for the free state and 256 scans for the bound state. NMR data were processed using NMRPipe software (Delaglio et al. 1995), and backbone resonances of GB1 in the free state were assigned using ^{1}H-^{15}N HSQC (Grzesiek and Bax 1993), ^{15}N TOCSY-HSQC, ^{15}N NOESY-HSQC (Marion et al. 1989), HNCA (Kay et al. 1990), and HN(CO)CA (Bax and Ikura 1991) with the NMRView software (Johnson and Blevins 1994)

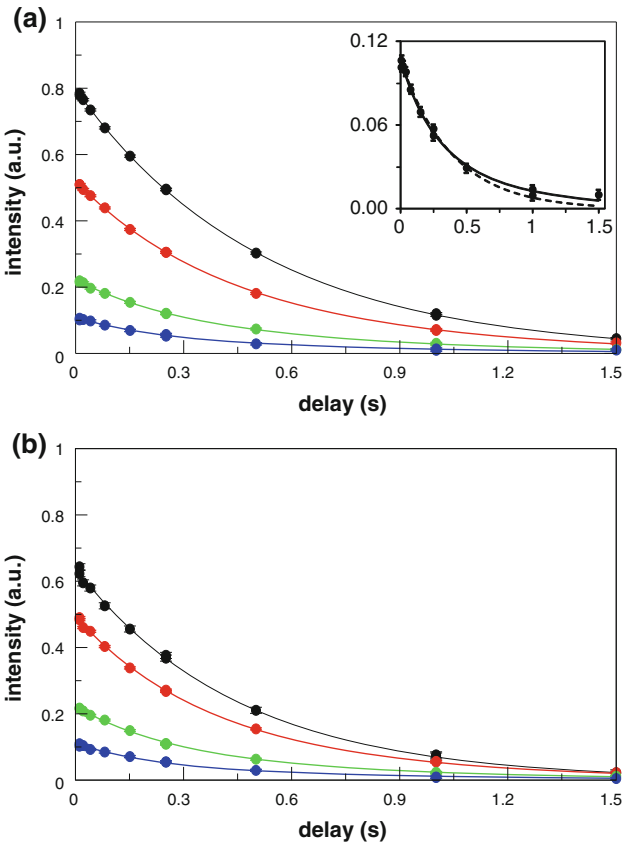

Fig. 2 ZZ-exchange profiles for GB1 residues Thr11 (**a**) and Ala34 (**b**) measured at GB1:IgG concentration ratios of 1:0 (*black*), 1:0.1 (*red*), 1:0.2 (*green*), and 1:0.3 (*blue*). The inset in (**a**) is a closed view of the profiles for the 1:0.3 sample fitted with Eq. 1 (*dashed line*) and Eq. 2 (*solid line*)

GB1–IgG interaction has no influence on the ZZ-exchange profiles. However, assessment of the goodness of fit by the reduced χ^2 value indicated that Eq. 2 was more appropriate than Eq. 1 (reduced $\chi^2 = 0.99$ versus 2.05), although the number of fitting parameters for Eq. 2 (4 global parameters + 6 local parameters × 55 residues) is smaller than that for Eq. 1 (8 local parameters × 55 residues). The inset in Fig. 2a shows that later points deviate more from the theoretical curve calculated with Eq. 1 than that calculated with Eq. 2. Moreover,
a comparison using Akaike's information criterion (Motulsky and Christopoulos 2004) indicated that the probability that Eq. 2 is likely to be correct is 1.00, with an evidence ratio of 1.26×10^{452} (the ratio of the probabilities of the equations) in favor of Eq. 2. Therefore, the ZZ-exchange profiles of free GB1 resonances are certainly perturbed by the interaction between GB1 and IgG.

The protein concentrations obtained in the ZZ-exchange experiment (Table 1) were in excellent agreement with those initially determined using UV/Vis spectroscopy (200 μM for GB1 and 0, 20, 40, and 60 μM for IgG). This agreement also supports the validity of the method. The auto-relaxation rates of the free and bound states and k_{on} and k_{off} rates were calculated from the ZZ-exchange curve fit. Figure 3 shows that the auto-relaxation rates of the bound state R_{1B} were determined with larger error bars than those of the free state R_{1F} because the R_{1F} rates were determined directly for the completely free form of GB1, whereas the R_{1B} rates were derived indirectly using Eq. 2. It should be noted that the regular ZZ-exchange method, which should require both signal intensities of two interconverting states (Farrow et al. 1994), can determine the auto-relaxation rates of both the free and bound states (Latham et al. 2009). Our ZZ-exchange method, of course, is applicable to the case in which bound resonances and exchange peaks are also observable. In such a case, accurate R_{1B} rates can be directly determined.

In order to further validate our ZZ-exchange method, we measured the dissociation constant using ITC. Figure 4 clearly shows that GB1 binds to IgG with a stoichiometric ratio of 0.5, indicating that GB1 binds to each of the two heavy chains in the Fc region of IgG. The K_D value obtained by the ZZ-exchange experiment (149 ± 34 nM) agrees reasonably well with that measured by ITC (59 ± 1.4 nM). The difference in the two experimentally

Table 1 ZZ-exchange curve fitting with a two-site exchange model

Parameter	Value from fitting (SD)[b]
$[GB1]_0$, μM	205 (9.3)
$[IgG]_0$, μM	22.8 (11)[a]
$k_{on} \times 10^7$, $M^{-1}\cdot s^{-1}$	1.50 (0.30)
k_{off}, s^{-1}	2.23 (0.12)
K_D, nM	149 (34.2)

[a] Determined for the 1:0.1 (GB1:IgG) sample. The concentrations of IgG in other samples with the GB1:IgG rations of 1:0, 1:0.2, and 1:0.3 were scaled by 0, 2, and 3, respectively

[b] Standard deviations (*SD*) were estimated by 100 Monte Carlo simulations

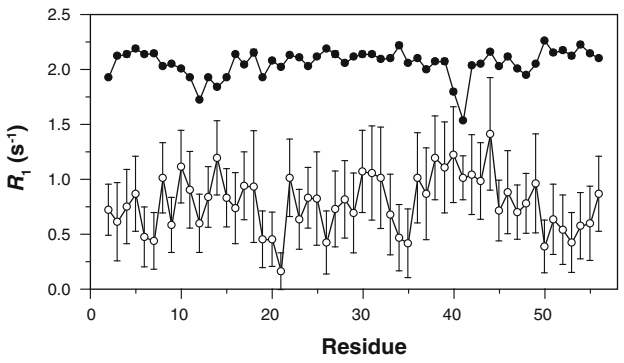

Fig. 3 Auto-relaxation R_1 rates of the free form (*filled circles*) and bound form (*open circles*) of [^{2}H,^{15}N]-GB1 as determined by ZZ-exchange curve fitting

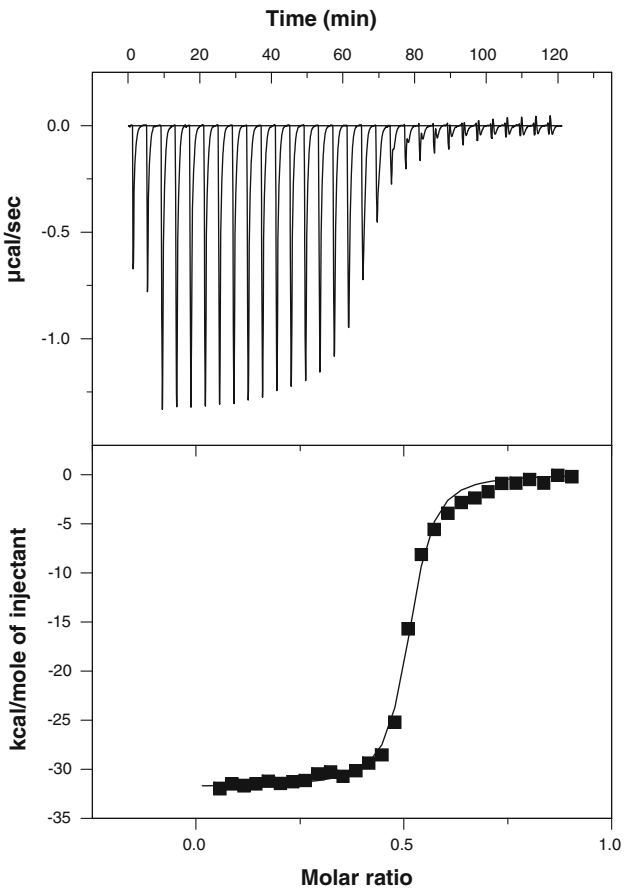

Fig. 4 ITC measurements of GB1 binding to IgG. The titration curve was fit with a two-state exchange model and the following thermodynamic parameters were determined: $K_D = 59 \pm 1.4$ nM, $\Delta H = -3.2 \pm 0.029$ kcal·mol^{-1}, and $\Delta S = -73 \pm 1.0$ kcal·mol^{-1}·K^{-1}

derived K_D values is on the same order as those determined in a previous R_2 dispersion study of the HIF-OH/TAZ1 interaction (Sugase et al. 2007b) (K_D of 143 nM as determined using the R_2 dispersion method, and K_D of 70 nM as determined using ITC). NMR methods tend to give larger dissociation constants (lower affinity) than ITC (Fielding et al. 2005). This is in part because NMR and ITC measure different properties of a system; ITC measures the thermal response of a ligand titration into a macromolecule under mechanical stirring, whereas an NMR experiment provides information regarding the solution composition of a system at equilibrium. Therefore, information obtained by NMR is averaged if there are minor states interconverting with the major states. The ZZ-exchange method (as well as the R_2 dispersion method) is sensitive to kinetic exchange rates rather than populations as shown in Eq. 2 and in the report by Sugase et al. (2007b). Consequently, it is possible that minor states rapidly interconverting with the free or bound states exist, such as an encounter complex or a different bound conformation. In the ITC experiments, an additional weak interaction was observed by ITC only in the presence of an excess of IgG from approximately 70 min in the titration. In an opposite titration in which GB1 (40 μM) in the syringe was titrated into IgG (600 μM) in the sample cell, the additional interaction was again detected in the presence of excess IgG (data not shown). Previously, Walker et al. determined a K_D of 306 nM for the interaction of GB1 and the isolated Fc fragment complex using fluorescence spectroscopy (Walker et al. 1995). Although this fluorescence method measures a different property than does NMR or ITC, the larger K_D value than those obtained using the whole IgG in the present study implies that the additional interaction can be ascribed to the binding of GB1 to the Fab region of IgG (Derrick and Wigley 1992). We neglected the additional weak interaction in ZZ-exchange curve fitting because all our ZZ-exchange experiments were conducted at much lower concentration ratios of IgG to GB1 than were used in the ITC experiments in which the additional interaction was observed. A very small amount of the additional weak interaction, however, might contribute to the ZZ-exchange profile, resulting in the larger K_D value.

We subsequently measured ^{15}N R_2 relaxation rates for the [^2H,^{15}N]-GB1:IgG sample at a concentration ratio of 1:0.3 using relaxation-compensated constant-time Carr-Purcell-Meiboom-Gill (CPMG) pulse sequences to test whether the GB1/IgG interaction can be analyzed by R_2 dispersion spectroscopy (Tollinger et al. 2001; Loria et al. 1999). The 1:0.3 concentration ratio sample was chosen because its exchange rate, which becomes faster as the amount of IgG increases, was the fastest, and therefore this sample would be the most likely to show R_2 dispersions. Figure 5, however, shows that no R_{ex} was observed, and

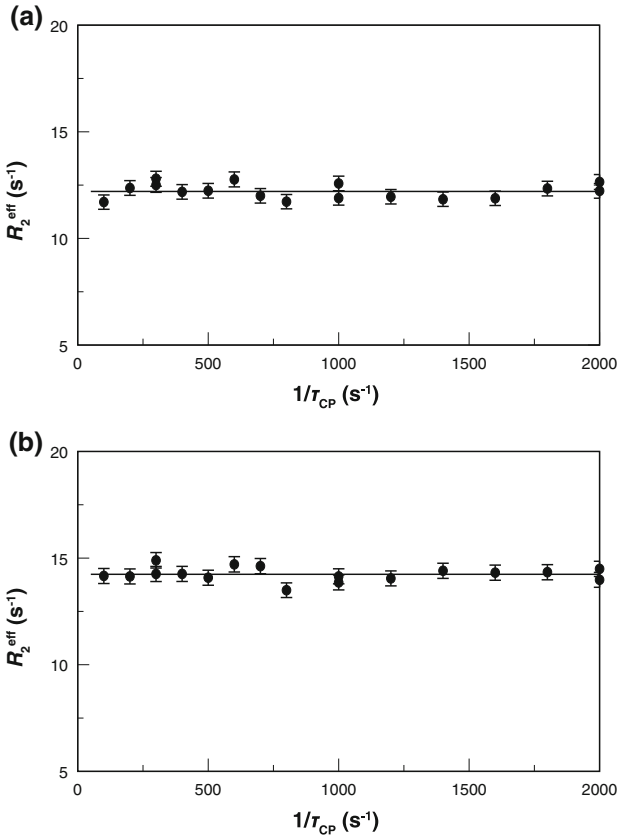

Fig. 5 ^{15}N R_2 dispersion profiles for GB1 residues Thr11 (**a**) and Ala34 (**b**) recorded using a Bruker BioSpin AVANCE DMX750 for [^2H,^{15}N]-GB1 in complex with IgG at a 1:0.3 concentration ratio. R_2 dispersion spectra were acquired as two-dimensional data sets with a constant relaxation delay of 40 ms using (1,024 × 128) complex points in the (t_2 × t_1) dimensions with 8 scans per t_1 increment and 3-s recycle delays. Four data points, including a reference spectrum acquired with the CPMG blocks omitted, were collected in duplicate and used to estimate the absolute uncertainties and the signal-to-noise ratio of each spectrum. The ^{15}N R_2 dispersion profiles were fit to the Carver and Richards equation (Carver and Richards 1972)

therefore the binding event could not be quantitated, The exchange rates k_{ex} (=[IgG Fc] k_{on} + k_{off}) were calculated to be at most 3.2 s^{-1} in the range of the IgG concentrations prepared for the ZZ-exchange experiments. Such an exchange rate is too slow for R_2 dispersion spectroscopy. Moreover, in the case of GB1, chemical shift changes upon binding to IgG should be small since GB1 is a rigid protein and does not appreciably change its conformation. The resulting small chemical shift changes could be another reason why R_{ex} rates were undetectable.

Previously, LaPlante et al. developed the transferred R_1 (or transferred T_1) method, in which relative changes in the R_1 relaxation rate of a ligand in the free state and in the presence of a very small amount of the target macromolecule are measured (LaPlante et al. 2000). This method is similar to our ZZ-exchange method but its application is limited to the condition of fast exchange. A major

difference between these two methods is their mathematical treatments for determining the dissociation constant from relaxation profiles. For the ZZ-exchange method, the dissociation constant is calculated from the binding kinetics k_{on} and k_{off} ($K_D = k_{off}/k_{on}$) as shown by Eq. 2. On the other hand, in the transferred R_1 experiment, the R_1 relaxation rate is measured as a population-averaged value of the free and bound states of a ligand:

$$R_{1av} = (1 - p_B)R_{1F} + p_B R_{1B} \quad (3)$$

where p_B represents the fraction of a ligand. This equation is valid only for the condition of fast exchange. The dissociation constant K_D is determined according to the equation:

$$K_D = [B]_0(1 - p_B)(1 - p_B[A]_0/[B]_0)/p_B \quad (4)$$

Equation 4 is derived from $K_D = [A][B]/[AB]$, that is, in the transferred R_1 experiment, the dissociation constant is calculated from the concentrations of the ligand and macromolecule. From another viewpoint, these equations indicate that the transferred R_1 method cannot determine k_{on} and k_{off} rates. It should also be noted that for the transferred R_1 method, the difference between R_{1F} and R_{1B} should be large enough to quantitate p_B accurately. In contrast, the ZZ-exchange method is applicable even in the case where the difference R_{1F} and R_{1B} is small if $[B]k_{on}$ and k_{off} perturb the ZZ-exchange profile sufficiently because the profile is defined by $[B]k_{on}$ and k_{off} as well as R_{1F} and R_{1B}, as shown by Eq. 2.

Other NMR methods, such as transferred R_2 (Su et al. 2007) and ^{1}H saturation transfer (Fawzi et al. 2010), can also be utilized to determine dissociation constants without observable bound resonances. The transferred R_2 method is similar to the transferred R_1 method (R_1 in Eq. 3 is replaced by R_2), and is more sensitive to ligand-macromolecule interactions than is the transferred R_1 method because the difference in the relaxation rate between the free and bound states is larger for R_2 than for R_1 if the complex is much larger than the ligand itself. However, the interaction to be analyzed must be sufficiently fast in order to prevent there being any contribution to the measured R_2 rate from chemical exchange between the free and bound states, and the exchange rate must be faster than the R_2 rate of the bound state (Su et al. 2007). Fawzi et al. used ^{1}H saturation transfer to determine the kinetics of amyloid β monomer-to-oligomer exchange (Fawzi et al. 2010). The ^{1}H saturation transfer method requires an assumption of the cross-relaxation rates of the monomer and the oligomer, and the R_2 rate(s) in the oligomer must be very large ($42{,}000 \pm 3000\ s^{-1}$ and $\sim 300\ s^{-1}$) in the case of amyloid β. In contrast, our ZZ-exchange method requires no assumption regarding NMR and kinetics parameters (except for the binding model, which is a common issue with other methods as well) as long as the exchange between the free and bound states sufficiently perturbs ZZ-exchange profiles in a concentration ratio-dependent manner.

Conclusion

Despite the absence of observable IgG-bound GB1 resonances, we derived the binding kinetics k_{on} and k_{off} and the auto-relaxation rates of GB1 in the free and bound states by analyzing the ZZ-exchange profiles of free GB1 resonances measured at four different GB1:IgG concentration ratios. As bound resonances of proteins are often unobservable or very broad due to high molecular weight, intermediate exchange, or aggregation at high concentrations, the ZZ-exchange method presented in this paper would be useful for studying a wide range of protein-protein, protein-nucleic acid, and protein-small molecule interactions, in particular those to which the R_2 dispersion method cannot be applied, such as very slow interactions and the binding of rigid proteins that undergo minimal conformational change.

Acknowledgments We thank Dr. Peter E. Wright (The Scripps Research Institute, San Diego, CA, USA) for providing the GB1 gene and the GLOVE program.

References

Angulo J, Enríquez-Navas PM, Nieto PM (2010) Ligand-receptor binding affinities from saturation transfer difference (STD) NMR spectroscopy: the binding isotherm of STD initial growth rates. Chem Eur J 16:7803–7812

Babine RE, Bender SL (1997) Molecular recognition of protein "ligand complexes: applications to drug design". Chem Rev 97:1359–1472

Bax A, Ikura M (1991) An efficient 3D NMR technique for correlating the proton and 15N backbone amide resonances with the α-carbon of the preceding residue in uniformly 15N/13C enriched proteins. J Biomol NMR 1:99–104

Carver JP, Richards RE (1972) General 2-site solution for chemical exchange produced dependence of T2 upon carr-purcell pulse separation. J Magn Reson 6:89–105

Dalvit C, Pevarello P, Tatò M, Veronesi M, Vulpetti A, Sundström M (2000) Identification of compounds with binding affinity to proteins via magnetization transfer from bulk water. J Biomol NMR 18:65–68

Dalvit C, Fogliatto G, Stewart A, Veronesi M, Stockman B (2001) WaterLOGSY as a method for primary NMR screening: practical aspects and range of applicability. J Biomol NMR 21:349–359

Delaglio F, Grzesiek S, Vuister GW, Zhu G, Pfeifer J, Bax A (1995) NMRPipe: a multidimensional spectral processing system based on UNIX pipes. J Biomol NMR 6:277–293

Derrick JP, Wigley DB (1992) Crystal structure of a streptococcal protein G domain bound to an Fab fragment. Nature 359:752–754

Eisenmesser EZ, Bosco DA, Akke M, Kern D (2002) Enzyme dynamics during catalysis. Science 295:1520–1523

Farrow NA, Zhang O, Forman-Kay JD, Kay LE (1994) A heteronuclear correlation experiment for simultaneous determination of ^{15}N longitudinal decay and chemical exchange rates of systems in slow equilibrium. J Biomol NMR 4:727–734

Fawzi NL, Ying J, Torchia DA, Clore GM (2010) Kinetics of amyloid β monomer-to-oligomer exchange by NMR relaxation. J Am Chem Soc 132:9948–9951

Ferreon JC, Lee CW, Arai M, Martinez-Yamout MA, Dyson HJ, Wright PE (2009) Cooperative regulation of p53 by modulation of ternary complex formation with CBP/p300 and HDM2. Proc Natl Acad Sci USA 106:6591–6596

Fielding L (2007) NMR methods for the determination of protein ligand dissociation constants. Prog Nucl Magn Reson Spectrosc 51:219–242

Fielding L, Rutherford S, Fletcher D (2005) Determination of protein–ligand binding affinity by NMR: observations from serum albumin model systems. Magn Reson Chem 43:463–470

Frederick KK, Marlow MS, Valentine KG, Wand AJ (2007) Conformational entropy in molecular recognition by proteins. Nature 448:325–330

Gronenborn AM, Filpula DR, Essig NZ, Achari A, Whitlow M, Wingfield PT, Clore GM (1991) A novel, highly stable fold of the immunoglobulin binding domain of streptococcal protein G. Science 253:657–661

Grzesiek S, Bax A (1993) The importance of not saturating H_2O in protein NMR. Application to sensitivity enhancement and NOE measurements. J Am Chem Soc 115:12593–12594

Johnson BA, Blevins RA (1994) NMRView: a computer program for the visualization and analysis of NMR data. J Biomol NMR 4:603–614

Karplus M (2010) Dynamical aspects of molecular recognition. J Mol Recognit 23:102–104

Karplus M, Kuriyan J (2005) Molecular dynamics and protein function. Proc Natl Acad Sci USA 102:6679–6685

Kay LE, Ikura M, Tschudin R, Bax A (1990) Three-dimensional triple-resonance NMR spectroscopy of isotopically enriched proteins. J Magn Reson 89:496–514

LaPlante SR, Aubry N, Déziel R, Ni F, Xu P (2000) Transferred ^{13}C T_1 relaxation at natural Isotopic abundance: a practical method for determining site-specific changes in ligand flexibility upon binding to a macromolecule. J Am Chem Soc 122:12530–12535

Latham MP, Zimmermann GR, Pardi A (2009) NMR chemical exchange as a probe for ligand-binding kinetics in a theophylline-binding RNA aptamer. J Am Chem Soc 131:5052–5053

Loria JP, Rance M, Palmer AG (1999) A relaxation-compensated Carr–Purcell–Meiboom–Gill sequence for characterizing chemical exchange by NMR spectroscopy. J Am Chem Soc 121:2331–2332

Ludwig C, Guenther UL (2009) Ligand based NMR methods for drug discovery. Front Biosci 14:4565–4574

Marion D, Driscoll PC, Kay LE, Wingfield PT, Bax A, Gronenborn AM, Clore GM (1989) Overcoming the overlap problem in the assignment of ^{1}H NMR spectra of larger proteins by use of three-dimensional heteronuclear ^{1}H-^{15}N Hartmann-Hahn-multiple quantum coherence and nuclear Overhauser-multiple quantum coherence spectroscopy: application to interleukin 1β. Biochemistry 28:6150–6156

Mayer M, Meyer B (1999) Characterization of ligand binding by saturation transfer difference NMR spectroscopy. Angew Chem Int Ed 38:1784–1788

Mayer B, Peters T (2003) NMR spectroscopy techniques for screening and indentifying ligand binding to proteins receptors. Angew Chem Int Ed 42:864–890

Motulsky H, Christopoulos A (2004) Fitting models to biological data using linear and nonlinear regression: a practical guide to curve fitting. Oxford University Press, New York

Ohlson S (2008) Designing transient binding drugs: a new concept for drug discovery. Drug Discov Today 13:433–439

Pervushin K, Riek R, Wider G, Wüthrich K (1997) Attenuated T_2 relaxation by mutual cancellation of dipole-dipole coupling and chemical shift anisotropy indicates an avenue to NMR structures of very large biological macromolecules in solution. Proc Natl Acad Sci USA 94:12366–12371

Redfern OC, Dessailly B, Orengo CA (2008) Exploring the structure and function paradigm. Curr Opin Struct Biol 18:394–402

Sauer-Eriksson AE, Kleywegt GJ, Uhlen M, Jones TA (1995) Crystal structure of the C2 fragment of streptococcal protein G in complex with the Fc domain of human IgG. Structure 3:265–278

Schulte-Herbrüggen T, Sørensen OW (2000) Clean TROSY: compensation for relaxation-induced artifacts. J Magn Reson 144:123–128

Su XC, Jergic S, Ozawa K, Burns ND, Dixon NE, Otting G (2007) Measurement of dissociation constants of high-molecular weight protein-protein complexes by transferred ^{15}N-relaxation. J Biomol NMR 38:65–72

Sugase K, Dyson HJ, Wright PE (2007a) Mechanism of coupled folding and binding of an intrinsically disordered protein. Nature 447:1021–1025

Sugase K, Lansing JC, Dyson HJ, Wright PE (2007b) Tailoring relaxation dispersion experiments for fast-associating protein complexes. J Am Chem Soc 129:13406–13407

Sugase K, Landes MA, Wright PE, Martinez-Yamout M (2008) Overexpression of post-translationally modified peptides in Escherichia coli by co-expression with modifying enzymes. Protein Expr Purif 57:108–115

Tollinger M, Skrynnikov NR, Mulder FA, Forman-Kay JD, Kay LE (2001) Slow dynamics in folded and unfolded states of an SH3 domain. J Am Chem Soc 123:11341–11352

Walker KN, Bottomley SP, Popplewell AG, Sutton BJ, Gore MG (1995) Equilibrium and pre-equilibrium fluorescence spectroscopic studies of the binding of a single-immunoglobulin-binding domain derived from protein G to the Fc fragment from human IgG_1. Biochem J 310:177–184